



Astrocyte-targeting therapy rescues cognitive impairment caused by neuroinflammation via the Nrf2 pathway

Akiko Nakano-Kobayashi^{a,b,1} , Andres Canela^c , Toru Yoshihara^d, and Masatoshi Hagiwara^{a,1}

Edited by Fred Gage, Salk Institute for Biological Studies, La Jolla, CA; received March 17, 2023; accepted July 6, 2023

Neuroinflammation is a common feature of neurodegenerative disorders such as Alzheimer's disease (AD). Neuroinflammation is induced by dysregulated glial activation, and astrocytes, the most abundant glial cells, become reactive upon neuroinflammatory cytokines released from microglia and actively contribute to neuronal loss. Therefore, blocking reactive astrocyte functions is a viable strategy to manage neurodegenerative disorders. However, factors or therapeutics directly regulating astrocyte subtypes remain unexplored. Here, we identified transcription factor NF-E2-related factor 2 (Nrf2) as a therapeutic target in neurotoxic reactive astrocytes upon neuroinflammation. We found that the absence of Nrf2 promoted the activation of reactive astrocytes in the brain tissue samples obtained from AD model 5xFAD mice, whereas enhanced Nrf2 expression blocked the induction of reactive astrocyte gene expression by counteracting NF- κ B subunit p65 recruitment. Neuroinflammatory astrocytes robustly up-regulated genes associated with type I interferon and the antigen-presenting pathway, which were suppressed by Nrf2 pathway activation. Moreover, impaired cognitive behaviors observed in AD mice were rescued upon ALGERNON2 treatment, which potentiated the Nrf2 pathway and reduced the induction of neurotoxic reactive astrocytes. Thus, we highlight the potential of astrocyte-targeting therapy by promoting the Nrf2 pathway signaling for neuroinflammation-triggered neurodegeneration.

neuroinflammation | neurotoxic reactive astrocytes | Nrf2

Astrocytes are the most abundant type of specialized glial cells in the central nervous system (CNS); they assist neurons in maintaining brain homeostasis. However, under neuroinflammatory conditions, astrocytes become “reactive” and contribute to CNS inflammation and neuronal loss (1). The neurotoxic reactive astrocytes are induced upon tumor necrosis factor (TNF)- α , interleukin (IL)-1 α , and complement component 1q (C1q) released from microglia. Neurotoxic reactive astrocytes have been detected in the brain tissue samples from patients with Alzheimer's disease (AD), Parkinson's disease, and multiple sclerosis (MS) (2). These findings suggest that neurotoxic reactive astrocytes play an important role in the pathogenesis of several neurological diseases; thus, blocking neurotoxic astrocytes conversion has been shown to help prevent or rescue the neurodegeneration observed in amyotrophic lateral sclerosis (ALS)-murine (3), Parkinson's disease (4), and AD models (5). To date, reactive astrocyte production can be inhibited by suppressing microglial activity (4, 5) or depleting microglial cytokine levels (3). However, direct targets or therapeutics to regulate neurotoxic reactive astrocytes have not been identified or developed, respectively.

A known key regulator of inflammation in CNS is the heterodimeric transcription factor (TF) nuclear factor (NF)- κ B (6), and activation of NF- κ B pathway is associated with various neurodegenerative conditions, including AD (7). In CNS-specific inhibitor of NF- κ B α (I κ B α) conditional knockout (KO) mice, with up-regulated NF- κ B pathway, one of the reactive astrocyte markers—complement C3 was overexpressed (8), suggesting the role of NF- κ B signaling in the generation or function of reactive neurotoxic astrocytes. Furthermore, inactivation of the astroglial NF- κ B pathway leads to functional improvement after spinal cord injury in the astrocyte-specific transgenic mice expressing a dominant negative form of I κ B α (9). These data indicate that the signaling cascade of NF- κ B in astrocytes can play a role in the pathogenesis of neurodegenerative disorders, such as AD. Given the importance of aberrant NF- κ B activation in neuroinflammatory conditions, it is important to elucidate how the astroglial NF- κ B pathway aggravates disease progression.

Based on previous studies, TF NF-E2-related factor 2 (Nrf2) is closely associated with the NF- κ B pathway. Nrf2 regulates the expression of hundreds of antioxidant genes to protect cells (10) and attenuates inflammation (11) by binding to the proximal end of the proinflammatory cytokine-encoding genes (12). Moreover, owing to the antioxidative and anti-inflammatory activities of Nrf2, it has been proposed as a potential target for the treatment of several neurodegenerative diseases; therapeutics targeting Nrf2 would function by inhibiting microglia-mediated neuroinflammation (13–15). Particularly in AD models,

Significance

Neurodegenerative disorders such as Alzheimer's disease (AD) impose increasing economic burden and threaten our aging societies; thus, effective therapies are urgently required owing to limited treatment options. To develop a cure for neurodegenerative disorders, we focused on “neurotoxic reactive astrocytes,” which induce neuronal death. Here, we identify the therapeutic target Nrf2 (NF-E2-related factor 2) that modulates neuroinflammation-triggered reactive astrocyte conversion. We found that reactive astrocytes were promoted in Nrf2-deleted brains of 5xFAD Alzheimer's disease mice and that Nrf2 pathway enhancement blocked the induction of reactive astrocytes by counteracting the NF- κ B subunit p65 recruitment. Importantly, treatment with ALGERNON2 potentiates the Nrf2 pathway and rescues the cognitive impairment observed in 5xFAD mice, indicating the potential of astrocyte-targeting therapy for neurodegenerative disorders.

Author contributions: A.N.-K. designed research; A.N.-K. and A.C. performed research; T.Y. contributed new reagents/analytic tools; A.N.-K. and A.C. analyzed data; T.Y. provided guide for behavioral test and critical comments; and A.N.-K., A.C., and M.H. wrote the paper.

The authors declare no competing interest.

This article is a PNAS Direct Submission.

Copyright © 2023 the Author(s). Published by PNAS. This article is distributed under [Creative Commons Attribution-NonCommercial-NoDerivatives License 4.0 \(CC BY-NC-ND\)](https://creativecommons.org/licenses/by-nc-nd/4.0/).

¹To whom correspondence may be addressed. Email: kobayashi.akiko.5e@kyoto-u.ac.jp or hagiwara.masatoshi.8c@kyoto-u.ac.jp.

This article contains supporting information online at <https://www.pnas.org/lookup/suppl/doi:10.1073/pnas.2303809120/-/DCSupplemental>.

Published August 7, 2023.

Nrf2 has been shown to either suppress oxidative stress/inflammation (16) or inhibit BACE1-mediated amyloid beta (A β) production (17); however, the role of astroglial Nrf2 in the regulation of NF- κ B or in reactive astrocyte production has not been established. In this study, we examined the role of Nrf2 in reactive astrocyte production in an AD murine model (5xFAD) to elucidate the potential of Nrf2 as an astrocyte-targeting therapeutic for AD.

Results

Nrf2 Affects the Induction of Neurotoxic Reactive Astrocyte in the AD Mouse Model. In the 5xFAD model, which overexpresses *APP* and *PSEN1* transgenes that possess a total of five familial AD-linked mutations (18), neuroinflammation is caused by accumulation of A β plaque and dysregulated cytokine production owing to inflammation triggers the induction of neurotoxic reactive astrocytes. In our study, we found that the expression of the genes encoding neurotoxic reactive astrocyte markers, namely *C3*, *H2-T23*, *H2-D1*, *Ggta1*, and *Iigp1*, was increased in the hippocampal tissue of 5xFAD murine brain in an age-dependent manner (Fig. 1A). To investigate the involvement of Nrf2 in reactive astrocyte induction under neuroinflammatory conditions, we evaluated the expression of reactive astrocyte marker genes in 5xFAD/Nrf2 KO mice (Nrf2^{-/-}). The up-regulated expression of reactive astrocytic marker genes was further exacerbated in the hippocampal tissues of Nrf2 KO 5xFAD mice (Fig. 1B). The expression of cytokines and the other astrocyte subtype markers such as *Clefl*, *Ptx3*, *S100a10*, *Cd109*, *Ptgs2*, *Emp1*, and *Tm4sf* was not affected in the Nrf2 KO mice (SI Appendix, Fig. S1), confirming that the involvement of Nrf2 was specific to the induction of neurotoxic reactive astrocytes. Moreover, amoeboid-shaped microglia exhibiting high Iba1 expression were accumulated in the A β -plaque regions of 5xFAD mice, and astrocytes with strong glial fibrillary acidic protein (GFAP) signals surrounded them (Fig. 1C, enlarged in subiculum). We observed that expression of C3 protein, a neurotoxic reactive astrocyte marker, was increased in the brain tissue samples of 5xFAD mice, and its expression was further enhanced in Nrf2 KO mice (Fig. 1C, Bottom). Note that neither amoeboid-shaped microglia nor astrocytes with high C3 expression were observed in the brain tissue samples of wild-type (WT) mice. Enhanced expression of Gbp2, another reactive astrocyte marker, was also confirmed in the hippocampal tissue of Nrf2 KO 5xFAD mice (Fig. 1D). Thus, it is indicated that Nrf2 is involved in the induction of neurotoxic reactive astrocytes in brain tissue exhibiting inflammation.

Nrf2 Regulates the Expression of Neurotoxic Reactive Astrocyte Genes. To elucidate the role of Nrf2 in astrocytes, we established primary astrocyte cultures and examined the role of the Nrf2 pathway in the expression of neurotoxic reactive astrocyte marker genes in vitro (Fig. 2A, scheme). Stimulation with Il-1 α /TNF- α /C1q (inflamm) induced the expression of neurotoxic reactive astrocyte marker genes *C3*, *H2-D1*, *Serping1*, and *Iigp1* (Fig. 2B) identified earlier (2). Nrf2 stabilizing reagents such as sulforaphane (SLF), diethylmaleate (DEM), and 15-deoxy- Δ 12,14-prostaglandin J2 (Δ 15-PGJ₂), which react with sulfhydryl (-SH) groups on Nrf2-tethering protein KEAP1 and enable Nrf2 to escape constant proteasomal degradation (SI Appendix, Fig. S2), suppressed the induction of neurotoxic reactive astrocyte marker genes (Fig. 2B). We confirmed that the intensity of C3 staining in astrocytes was up-regulated upon inflamm treatment, which was suppressed by the SLF treatment (Fig. 2C). Thus, the stabilization of Nrf2 protein can inhibit the expression of reactive astrocyte markers.

To further clarify the specific involvement of Nrf2 in the expression of reactive astrocyte marker genes, we prepared primary

astrocytes from Nrf2 KO mice and assessed the expression of neurotoxic reactive astrocyte marker genes. We found that the induction of *H2-D1*, *Serping1*, and *Iigp1* expression upon inflamm stimulation was exacerbated in the Nrf2 KO astrocytes (Fig. 2D), indicating the involvement of Nrf2 in the neurotoxic reactive astrocyte marker gene expression. The up-regulated expression of reactive astrocyte markers *C3*, *Gbp2*, and *Qa1* (product of *H2-T23* gene) was also confirmed at the protein level (Fig. 2E); thus, these data established that Nrf2 regulates the expression of neurotoxic reactive astrocyte marker genes.

To exclude microglia from astrocyte cultures, we differentiated astrocytes from induced pluripotent stem cells (iPSCs) by preventing mesodermal differentiation toward microglia (Fig. 2F, scheme). We found that the expression of the reactive astrocyte marker genes *C3* and *HLA-A* (corresponding to murine *H2-D1* gene) was up-regulated in response to neuroinflammatory stimuli, which was down-regulated in the presence of Nrf2 inducers in these astrocytes generated from human iPSCs (Fig. 2F). Thus, our data indicate that Nrf2 induction regulates the gene expression of neurotoxic reactive astrocyte markers due to neuroinflammatory stimuli in both murine and human astrocytes.

Nrf2 Suppresses the NF- κ B Pathway and Regulates the Conversion of Reactive Astrocytes. Next, we investigated the influence of Nrf2 on NF- κ B, the TF responsible for inflammation, since identified reactive astrocyte-inducing cytokines, Il-1 α and TNF α (2), drive NF- κ B downstream pathway in common. First, we examined whether the NF- κ B cascade is involved in the induction of neurotoxic reactive astrocyte marker genes using inhibitors of the NF- κ B pathway. We found that the induction of the marker genes upon inflamm stimulation was blocked by the I κ B kinase (IKK) inhibitors TPCA-1, Bay11-7082, BOT-46, and BMS345541, which inhibit the IKK complex and suppress the activation of NF- κ B downstream pathway, in a dose-dependent manner (SI Appendix, Fig. S3A). Downregulation of the C3 protein by the inhibition of the NF- κ B pathway was also confirmed in primary astrocyte cultures (SI Appendix, Fig. S3B).

Nrf2 in macrophages suppresses the expression of proinflammatory cytokines by binding to the proximal end of their promoters (12). To investigate whether Nrf2 directly binds to the neurotoxic reactive astrocyte marker gene locus, we performed chromatin immunoprecipitation (ChIP)-sequencing (seq) analyses of Nrf2 and p65 (Fig. 3A) from the astrocytes treated with inflamm cytokines in the presence of vehicle (DMSO) or the Nrf2-inducer SLF to determine whether these factors bind to the marker gene loci. At the transcription start site (TSS) of *C3*, the peaks of chromatin immunoprecipitated (ChIPed) p65- and Nrf2-associated reads were found to be accumulated under inflammatory conditions, indicating that p65 and Nrf2 were recruited to the TSS adjacent region of *C3* in response to inflammatory stimuli (Fig. 3A). We observed that SLF treatment recruited Nrf2 to these regions, and the accumulation of the p65-associated read-peaks at the TSS region was reduced when the astrocytes were cotreated with SLF (Fig. 3A). Similar observations were made for the loci of other reactive astrocyte marker genes, such as *H2-D1* and *Gbp2* (Fig. 3A). A reduction in p65-associated read-peaks upon SLF treatment was more evident in the aggregate plot at the p65-binding motif (Fig. 3B). The p65-associated read-peaks displayed a sharp summit upon treatment with inflamm cytokines (a deep blue line); the read-peak heights were reduced following cotreatment with SLF (SLF.inflamm, a blue line). We also observed an increase in the number of Nrf2-associated read-peaks under the SLF.inflamm condition (an orange line) compared to those under the SLF.NT condition (a yellow line, NT; nontreated), despite the center axis of the aggregate plot being at

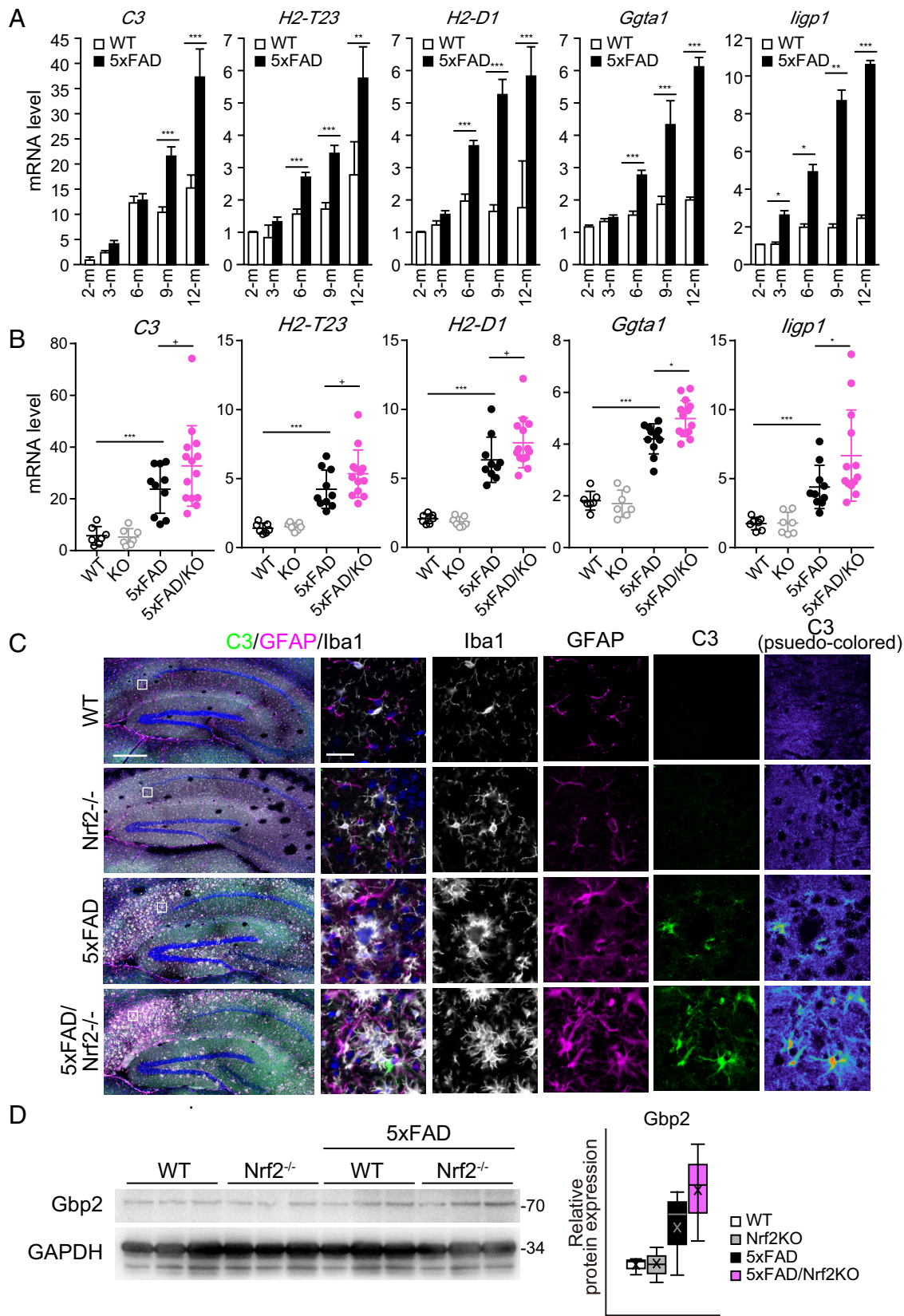


Fig. 1. Neurotoxic reactive astrocytes in 5xFAD AD mouse model. (A) mRNA levels of reactive astrocyte marker genes in the hippocampal tissue samples of 5xFAD mice at 3, 6, 9, and 12 mo of age and corresponding WT mice. Two-month-old mice served as control. N = 3 for WT, N = 3 for 5xFAD at 3-mo-old, and N = 6 for 6-, 9-, and 12-mo-old 5xFAD mice. Error bars indicate SEM. *** $P < 0.001$ (compared between corresponding age groups, Student's t test). (B) Quantification of mRNA expression of neurotoxic reactive astrocyte marker genes in the hippocampal-tissue samples of 5xFAD/Nrf2 KO mice. Age: 8-mo-old; WT: N = 7; Nrf2KO: N = 7; 5xFAD: N = 11; 5xFAD/Nrf2KO: N = 14. * $P < 0.05$, ** $P < 0.01$, *** $P < 0.001$, and + $P < 0.1$ (Tukey–Kramer multiple comparison test). Error bars indicate SEM. (C) Representative images of the hippocampal-tissue samples of 5xFAD/Nrf2 KO. The regions indicated with white squares in the subiculum are enlarged on the *Right*. To visualize the fluorescent intensity, C3 staining is shown in pseudocolored on the *Right* side. (Scale bars: 400 μm and 20 μm .) (D) Western blotting analysis of hippocampal tissue samples using the indicated antibodies. Tissues from three animals were analyzed for each genotype. The box plots on the *Right* indicate the protein expression levels.

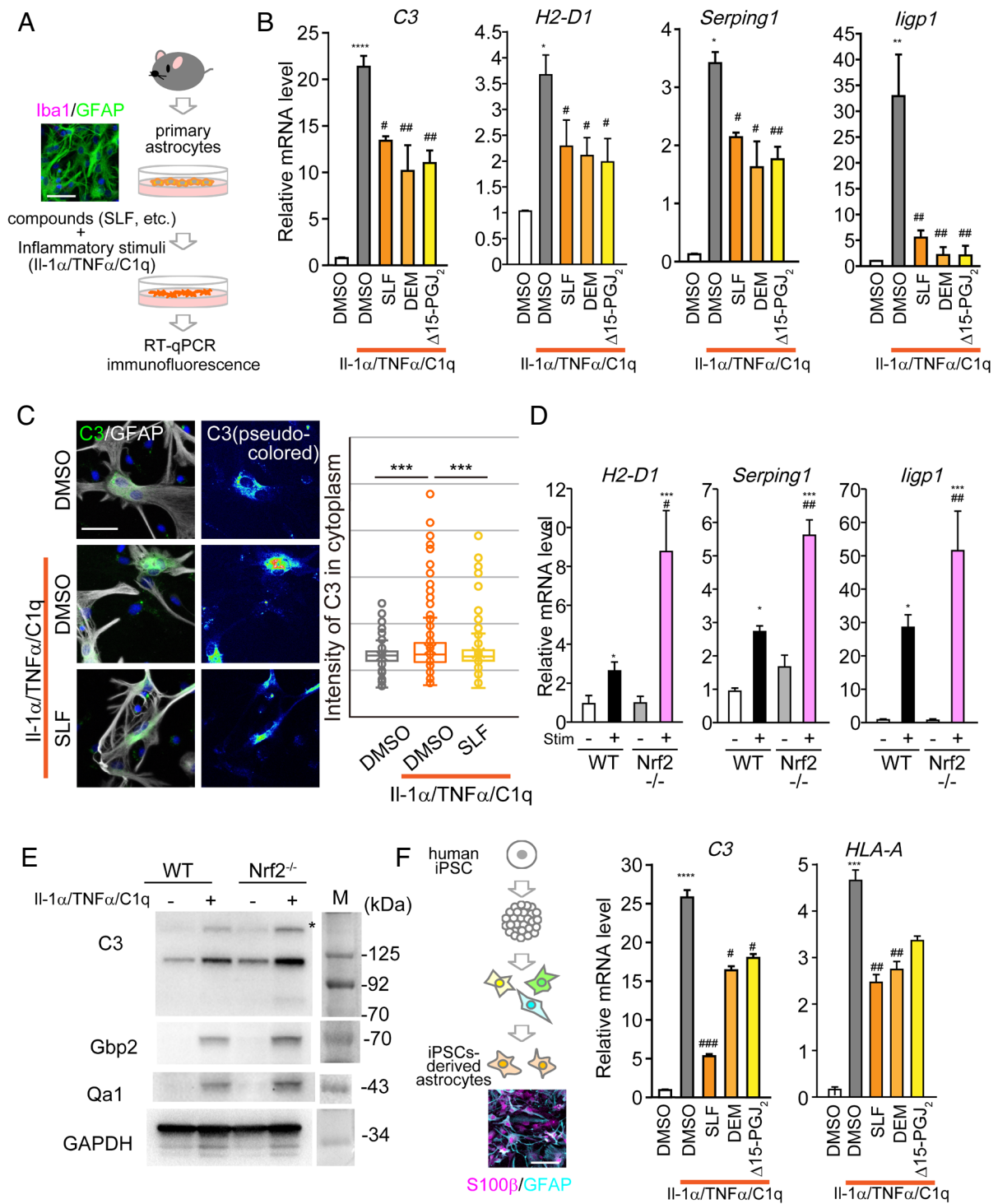


Fig. 2. Nrf2 regulates gene expression of reactive astrocytes. (A) Experimental scheme: Primary astrocytes were isolated and stimulated with Il-1 α /TNF α /C1q, followed by gene expression analysis using RT-qPCR or immunofluorescence. A representative image of cultures is shown on the *Left*. (Scale bar, 50 μ m.) (B) Quantification of the relative mRNA level of each gene in astrocytes stimulated with Il-1 α /TNF α /C1q and DMSO or Nrf2-inducing compounds for 4 h. * P < 0.05 and **** P < 0.0001 compared to unstimulated control; # P < 0.05 and ## P < 0.01 compared to stimulated/DMSO-treated control (Tukey-Kramer multiple comparison test). Error bars indicate SEM. (C, *Left*) Representative images of primary astrocytes stained with anti-C3 and anti-GFAP antibodies. *Right* panel: pseudocolored C3 to visualize the intensity of C3 protein expression. (Scale bar, 10 μ m.) The quantitative box plots are shown on the *Right*. *** P < 0.001. (D) Quantification of the relative mRNA level of each gene expression in astrocytes prepared from WT or Nrf2 KO (-/-) mice, stimulated with IL-1 α /TNF α /C1q for 4 h. * P < 0.05 and *** P < 0.001 versus unstimulated control in each genotype; # P < 0.05 and ## P < 0.01 versus the stimulated WT control (Tukey-Kramer multiple comparison test). Error bars stand for SEM. (E) Western blot analysis of protein isolated from astrocytes prepared from WT or Nrf2^{-/-} mice after Il-1 α /TNF α /C1q stimulation for 24 h. The protein size marker is indicated on the *Right*. The bands corresponding to full-length C3 are marked with an asterisk (*). The bands at 110 kDa and at 70 kDa correspond to α chain of C3 and iC3b, respectively. (F, *Left*) Experimental scheme. Astrocyte cultures were generated for assays from human iPSCs. A representative image stained with astrocyte markers S100 β and GFAP is shown. (Scale bar, 100 μ m.) *Right*: Quantification of the relative mRNA level of each gene in human iPSCs-derived astrocytes stimulated with Il-1 α /TNF α /C1q and indicated Nrf2-inducing compounds for 24 h. * P < 0.05 and *** P < 0.001 versus unstimulated control; ## P < 0.01 and ### P < 0.001 compared to stimulated/DMSO-treated control (Tukey-Kramer multiple comparison test). Error bars indicate SEM.

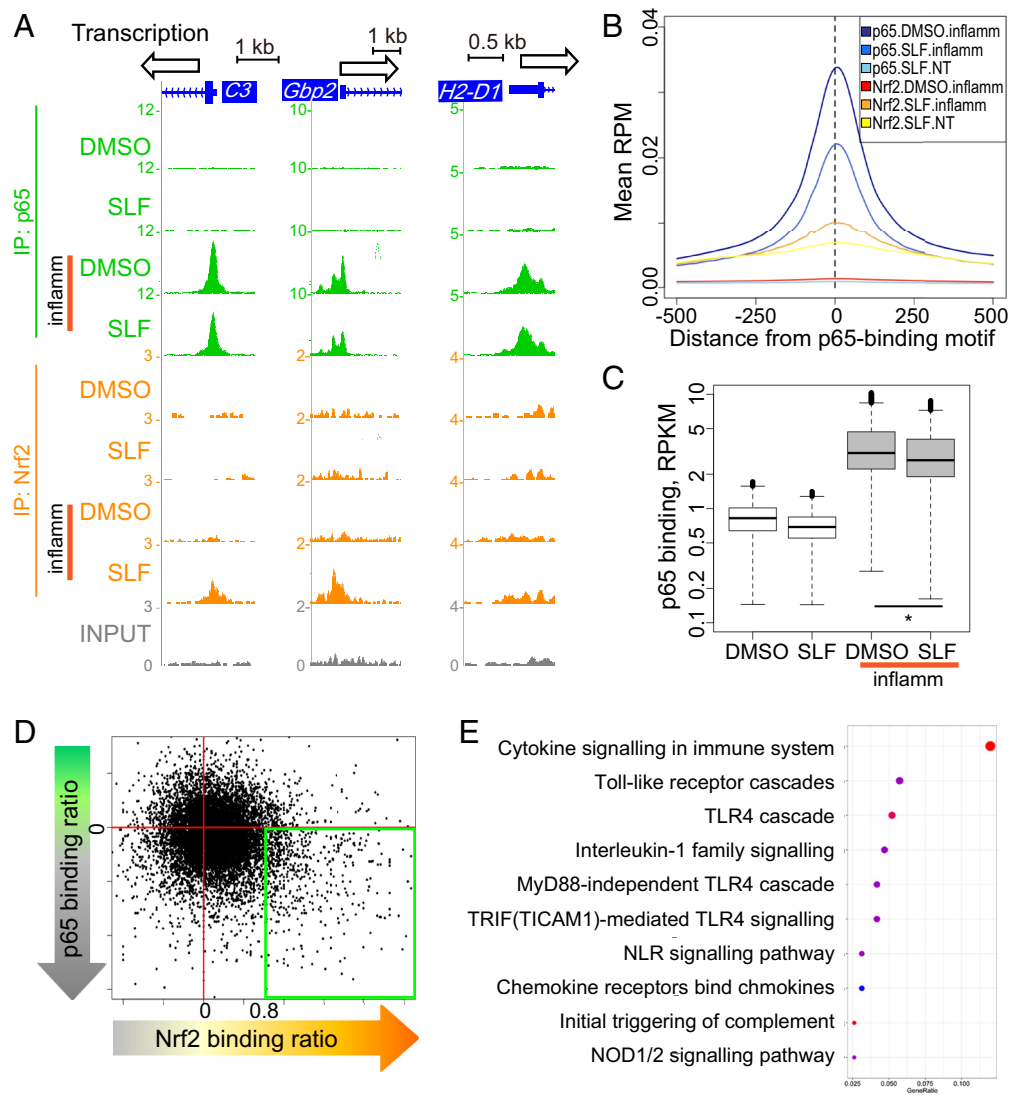


Fig. 3. Nrf2 counteracts the NF- κ B pathway and regulates the conversion of reactive astrocytes. (A) ChIP-seq profiles at the TSS site of indicated genes. Exons are shown as navy-blue squares, and box arrows represent the direction of transcription. inflamm stands for IL-1 α /TNF α /C1q stimulation. (B) Aggregate plots of indicated peaks at the p65 binding motif. (C) The box plots of p65-binding peaks at regions where p65 peaks overlapped with enhancers (H3K27Ac⁺) in each condition. * $P < 0.05$. (D) The scatter plot of the common peaks of p65 and Nrf2 binding based on “binding ratio” calculated as SLF.inflamm over DMSO.inflamm and SLF.inflamm over SLF.NT, respectively. Red lines indicate zero. The genes surrounded with a green square were used for Fig. 3E. (E) GO analysis of the genes with p65-binding ratio less than zero and Nrf2-binding ratio more than 0.8 (a green square in Fig. 3D).

the p65-binding motif, implicating that Nrf2 binds to the adjacent TSS regions of reactive marker genes and inhibits p65 recruitment under neuroinflammatory conditions. We also observed changes in p65-binding at the enhancer regions under SLF treatment, as shown in the box plots of Fig. 3C, indicating that SLF treatment reduced the p65-binding read-peaks upon cytokine treatment. To further elucidate the correlation between the binding of p65 and Nrf2 around the TSS regions, we extracted the common read-peaks of p65 and Nrf2 obtained under inflammatory conditions (both DMSO and SLF), calculated the “binding ratio” as SLF.inflamm over DMSO.inflamm and SLF.inflamm over SLF.NT, respectively, and then plotted the binding ratio of p65 and Nrf2 to compare the common read-peaks under inflammatory conditions with and without SLF treatment (Fig. 3D). We observed that the population of common read-peaks was largely distributed in the region where the Nrf2-binding ratio was higher than 0 and the p65-binding ratio was lower than 0 (lower right quadrant, shown with red lines in Fig. 3D), indicating that the more the Nrf2-binding, the lesser the p65-binding. We extracted genes with p65-binding peaks in a ratio < 0 and Nrf2-binding peaks in a ratio > 0.8 (indicated with a green square in Fig. 3D) upon SLF treatment. To determine which pathway is regulated by p65 and Nrf2, we performed gene enrichment analysis of the extracted genes (Fig. 3E). Gene Ontology (GO) analysis revealed that these genes were enriched in the following pathways: the cytokine signaling in the immune system, Toll-like

receptor cascades, and IL-1 family signaling, suggesting the contribution of astrocytes in neuroinflammation. Moreover, the previously reported pan-reactive marker genes (*STEAP4*, *Lcn2*, and *Serpina3h*) and the neurotoxic reactive astrocyte marker gene *Gbp2* were in the top 30 extracted genes (SI Appendix, Table S1). Collectively, these data conclude that Nrf2 regulates the gene expression of reactive astrocyte markers by suppressing p65-binding at their TSS regions under neuroinflammatory conditions.

Astrocytes Express Interferon (IFN)-I and Antigen-Presenting Pathway Genes upon Neuroinflammatory Stimuli, Which Is Suppressed by Nrf2. Next, we examined the expression of genes with increased Nrf2- and reduced p65-binding to their TSS regions in astrocytes stimulated with inflamm cytokines. Therefore, we performed nascent RNA-seq by labeling the newly transcribed products with 5-ethynyl uridine (EU) of astrocytes, during stimulation (Fig. 4A). Nascent RNA profiles clearly indicated that reactive astrocyte genes such as *C3*, *H2-D1*, and *Gbp2* were robustly transcribed upon stimulation and that this up-regulated transcription was suppressed upon cotreatment with SLF (SI Appendix, Fig. S4A). Genes identified by ChIP-seq that reduced p65-binding with SLF treatment such as *Gbp5*, *Cxcl11*, and *Tnfrsf3* (listed in SI Appendix, Table S1) also showed robust upregulation in nascent transcripts upon inflammatory stimuli, which was suppressed by SLF cotreatment (SI Appendix, Fig. S4B).

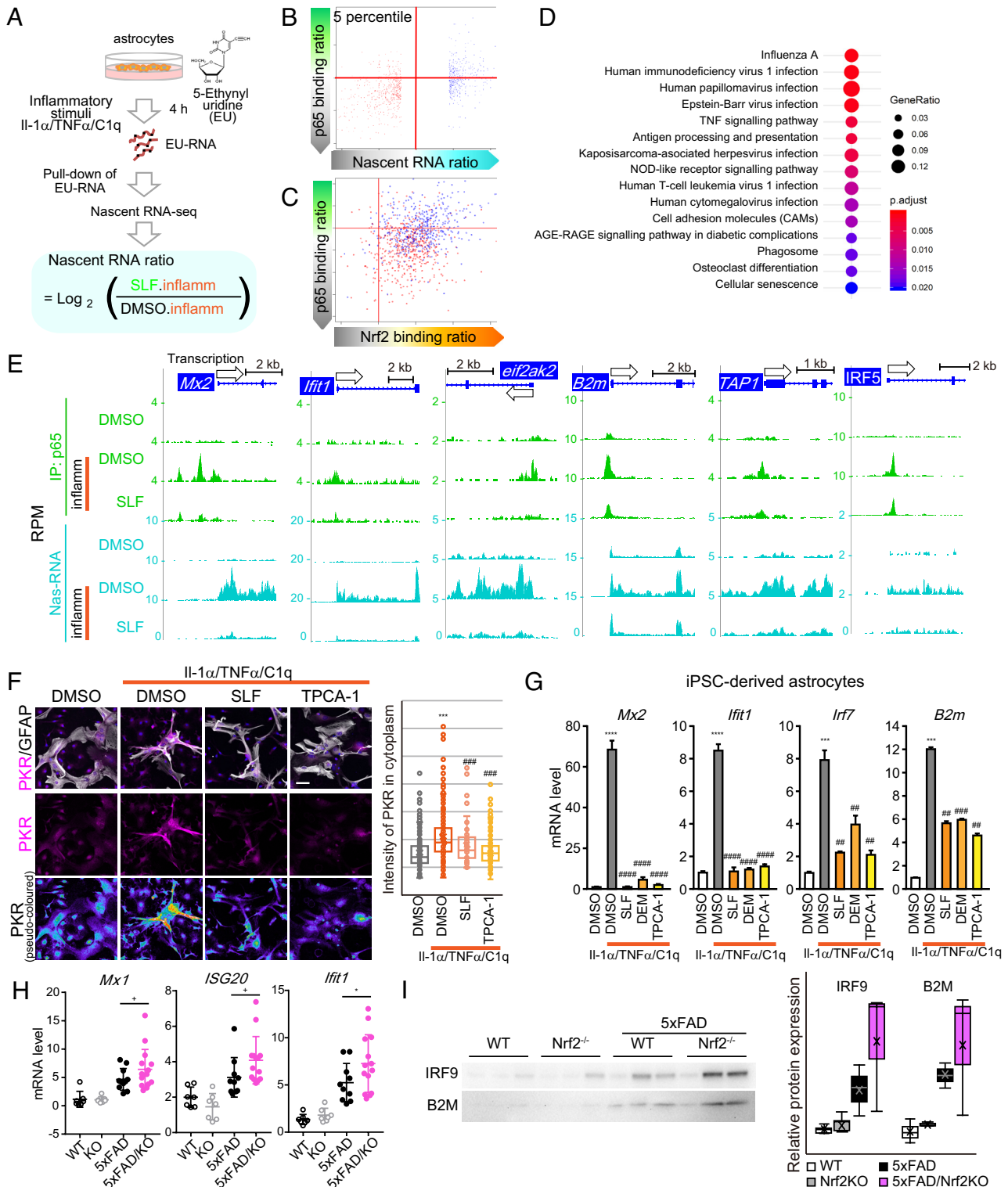


Fig. 4. Gene expression profiles in neuroinflammatory astrocytes. (A) Experimental scheme: Nascent transcripts in stimulated astrocytes were labeled with EU during the stimulation with IL-1 α /TNF α /C1q (inflammatory stimuli, inflamm), followed by pulled-down and seq. The nascent RNA ratio was calculated based on the RPKM value under the SLF.inflamm condition compared to those under the DMSO.inflamm condition. (B) Nascent RNA ratio was plotted based on the p65-binding ratio (Fig. 3D). Down- and up-regulated genes in the top five percentiles are colored in red and in blue, respectively. Red lines indicate zero. (C) Scatter plot comparing Nrf2- and p65-binding ratio (Fig. 3D) was replotted with color indication of five percentiles determined using the nascent RNA ratio. Red lines indicate zero. (D) KEGG pathway analysis of the five percentile genes less transcribed under the SLF.inflamm condition (indicated in red color) compared to those under the DMSO.inflamm condition. (E) Examples of the profiles of p65 ChIP-seq and nascent RNA-seq of less transcribed genes under the SLF.inflamm condition. Exons are shown as navy-blue squares, and box arrows represent the direction of transcription. inflamm stands for Il-1 α /TNF α /C1q stimulation. (F) Representative images of astrocytes stained with anti-PKR and anti-GFAP antibodies. The *Bottom* panels show pseudocolored PKR. (Scale bar = 50 μ m.) Quantification of the signal intensity of PKR fluorescence in astrocytes is shown on the *Right*. (G) Quantification of indicated mRNA expression in iPSC-derived astrocytes. **** P < 0.001, **** P < 0.0001, *** P < 0.001 (compared to the unstimulated condition), ## P < 0.01, ### P < 0.001, and ##### P < 0.0001 (compared to the stimulated control) (Tukey-Kramer multiple comparison test) Error bars indicate SEM. (H) Quantification of the mRNA level in the hippocampal tissues of indicated mice. WT; N = 7, KO; N = 7, 5xFAD; N = 11, 5xFAD/KO; N = 14. Error bars indicate SEM. + P < 0.1 (Tukey-Kramer multiple comparison test). (I) Western blot analysis (re-probed from Fig. 1D) using the indicated antibodies in the hippocampal tissues of indicated animals. The box plots on the right indicate the protein expression levels.

Note that genes of other subtypes known as “pan-reactive” (*Lcn2*, *Vim*, and *Gfap*) and “A2” (*Cclf1*, *Ptx3*, and *Sphk1*) astrocytes showed p65 accumulation upon treatment with inflamm cytokines; however, the cotreatment with SLF did not induce significant reduction in p65-binding nor nascent RNA (*SI Appendix*, Fig. S5). To understand the correlation between p65-binding and the p65-bound gene expression in inflamm conditions with/without SLF treatment, we calculated the “Nascent RNA ratio” in reads per kilobase of exon per million reads mapped (RPKM) of nascent transcripts under the SLF.inflamm condition over those under the DMSO.inflamm condition (SLF.inflamm/DMSO.inflamm, Fig. 4A) and then plotted the Nascent RNA ratio with the “p65 binding ratio” calculated from the data obtained by ChIP-seq of p65. To focus on the down-regulated genes under SLF treatment, we extracted the genes in the top five percentile based on RNA ratio (Fig. 4B, colored in red for the down-regulated genes). We observed that the genes in the top five percentile less transcribed upon SLF treatment (listed in *SI Appendix*, Table S2) were distributed below zero on the y-axis of the p65-binding ratio plot, which indicates reduced p65-binding under the SLF.inflamm condition. This finding suggests that the reduced expression of the genes is correlated to reduced p65-binding. We highlighted the genes in these five percentiles using the plot of p65/Nrf2 binding ratio (Fig. 3D) to further confirm the correlation between their expression and p65-binding. These two populations are separately distributed; the five percentiles of less transcribed genes under the SLF.inflamm condition (colored in red) exhibited increased Nrf2-binding and decreased p65-binding (Fig. 4C), suggesting that the genes with increased Nrf2-binding under the SLF.inflamm condition had reduced number of p65-binding peaks and smaller newly transcribed population (marked with a red color). To elucidate the pathways regulated by p65/Nrf2, we performed the Kyoto Encyclopedia of Genes and Genomes (KEGG) enrichment analysis for the genes less transcribed in the top five percentile; the genes were enriched in the pathways for virus infection and antigen presentation (Fig. 4D). Notably, the KEGG analysis of nascent gene expression matched well with the GO analysis of the genes extracted from Nrf2/p65 ChIP-seq (Fig. 3E), strongly suggesting that Nrf2/p65 regulate the expression of reactive astrocyte marker genes under neuroinflammatory conditions.

To model the reactive astrocytes for ChIP-seq/Nascent RNA-seq analyses in vitro, we utilized inflammatory cytokines, namely, IL-1 α /TNF α /C1q, which was determined to induce A1 astrocytes previously (2). However recent advances in single-cell seq techniques have revealed that there are diverse astrocyte subtypes contrary to the two-dimensional A1/A2 classification (19), and at least six astrocytic transcriptomic clusters were described in the hippocampi of 7-mo-old 5xFAD mice (20). To gain more insights into the reactive astrocytes genes regulated by NF- κ B/Nrf2 determined in our study, especially “disease-associated astrocytes (DAA)”, we extracted genes from cluster 4 (GFAP-high “DAA”) in comparison to clusters 1 and 2 (GFAP-low “homeostatic astrocytes”) (20) and then plotted onto our data of the ratio DMSO.inflamm over DMSO.NT. (*SI Appendix*, Fig. S6A). Our analysis showed that the p65 binding was up-regulated upon inflamm stimulation, as most of the genes were distributed above zero, implying that DAA genes (highlighted in red in *SI Appendix*, Fig. S6A) seem to be regulated by the NF- κ B pathway in cultured astrocytes stimulated upon inflamm stimuli. To further elucidate the overlap with SLF-treated conditions, DAA genes were merged with the plot in Fig. 3D (p65/Nrf2 binding ratio calculated from SLF.inflamm over DMSO.inflamm) and the plot in Fig. 4B (p65 binding ratio/Nascent RNA ratio). Consistent with the results of Habib et al. (20), some of the DAA genes overlapped (marked in red in *SI Appendix*, Fig. S6B) with the reactive astrocyte genes that

were up-regulated upon inflamm cytokine stimulation (*SI Appendix*, Fig. S6B). Additionally, some DAA genes seemed to be regulated by the Nrf2 axis as shown in *SI Appendix*, Fig. S6C that 25 out of 237 DAA genes overlapped with five percentile genes that were down-regulated upon cotreatment with SLF. For examples, the gene expression of *ApoE* did not change upon inflamm stimulation, and recruitment of p65 at the TSS locus was not observed. The recruitment of p65 upon inflamm cytokines was observed in *CLU*, *Cst3*, and *Fth1* genes at TSS loci, but their expression levels were not up-regulated. *Chil1* and *Aqp4* genes are likely regulated by the Nrf2-dependent pathway (all shown in *SI Appendix*, Fig. S6D). Thus, genes in the DAA subtype undergo various regulation including the NF- κ B/Nrf2 axis.

We noticed that the down-regulated genes (top five percentile) included genes from the IFN-I and antigen presentation pathways, such as *Mx2* (interferon-induced GTP-binding protein Mx2), *IRF5* (interferon regulatory factor 5), *EIF2AK2* (eukaryotic translation initiation factor 2-alpha kinase 2; coding for PKR, double-stranded RNA-activated protein kinase), β -2-microglobulin (*B2m*), and *Tap1* (Transporter 1) (*SI Appendix*, Table S2). We observed the accumulation of the p65 peaks at the TSS region upon cytokine stimulation, which was reduced by cotreatment with SLF (green-colored in Fig. 4E). Corroborating with these observations, the transcription rate of these genes was increased under the DMSO.inflamm condition but suppressed when cotreated with SLF (turquoise-colored in Fig. 4E). We confirmed that the expression of the translated products of these genes, i.e., PKR, B2M, TAP1, and IRF9, was induced upon inflammatory stimuli with inflamm cytokines and suppressed by SLF treatment or TPCA-1 treatment (Fig. 4F and *SI Appendix*, Fig. S3C).

Next, we investigated the induction of these genes under neuroinflammatory conditions in human astrocytes derived from iPSCs. We found that the expression of IFN-I genes (*Mx2*, *Ifit1*, and *Irf7*) and the antigen-presenting pathway gene *B2m* was up-regulated upon inflamm cytokine stimulation, which was suppressed by cotreatment with Nrf2 inducers (SLF and DEM) or the NF- κ B pathway inhibitor TPCA-1 (Fig. 4G). These results indicate that SLF treatment can suppress the expression of genes associated with IFN-I and the antigen-presenting pathway in human and murine astrocytes upon neuroinflammatory stimuli.

We also examined whether these genes were up-regulated in the brain tissue samples of 5xFAD mice. We found age-dependent increase in the expression of antigen-presenting genes (*Tap1* and *B2m*) and IFN-I-related genes (*Mx1*, *Ifit1*, *Irf5*, *Irf7*, *Irf9*, and *EIF2AK2*) (*SI Appendix*, Fig. S7). Furthermore, the up-regulated gene expression was exacerbated in the hippocampal tissues of the Nrf2 KO 5xFAD mice (Fig. 4H and I). Thus, it is evident that reactive astrocytes express IFN-I genes and antigen-presenting genes and that Nrf2 is involved in the regulation of the induction of these reactive astrocyte marker genes in neuroinflammatory brains.

Potentiating the Nrf2 Pathway Can Suppress the Neuroinflammation-Triggered Neurotoxic Reactive Astrocytes and Relieve Impaired Brain Function in the AD Mouse Model. To explore the possibility of astrocyte-targeting therapy for neuroinflammation-triggered neurodegeneration, we examined whether the brain dysfunction caused by neuroinflammation can be rescued by the potentiation of the Nrf2 pathway. We administered ALGERNON2 (ALG2), an Nrf2 pathway-potentiating chemical that costabilizes p21/Nrf2, as previously reported (15), to 3-mo-old 5xFAD mice and assessed the conversion of reactive astrocytes in the hippocampus of 10-mo-old WT and 5xFAD mice. We found that the treatment with ALG2 reduced the expression of *C3*, *Ifit1*, *IRF5*, *Tap1*, and *B2m* in the hippocampal tissue of 5xFAD mice compared to that in the WT mice (Fig. 5A). We observed that C3 was localized in

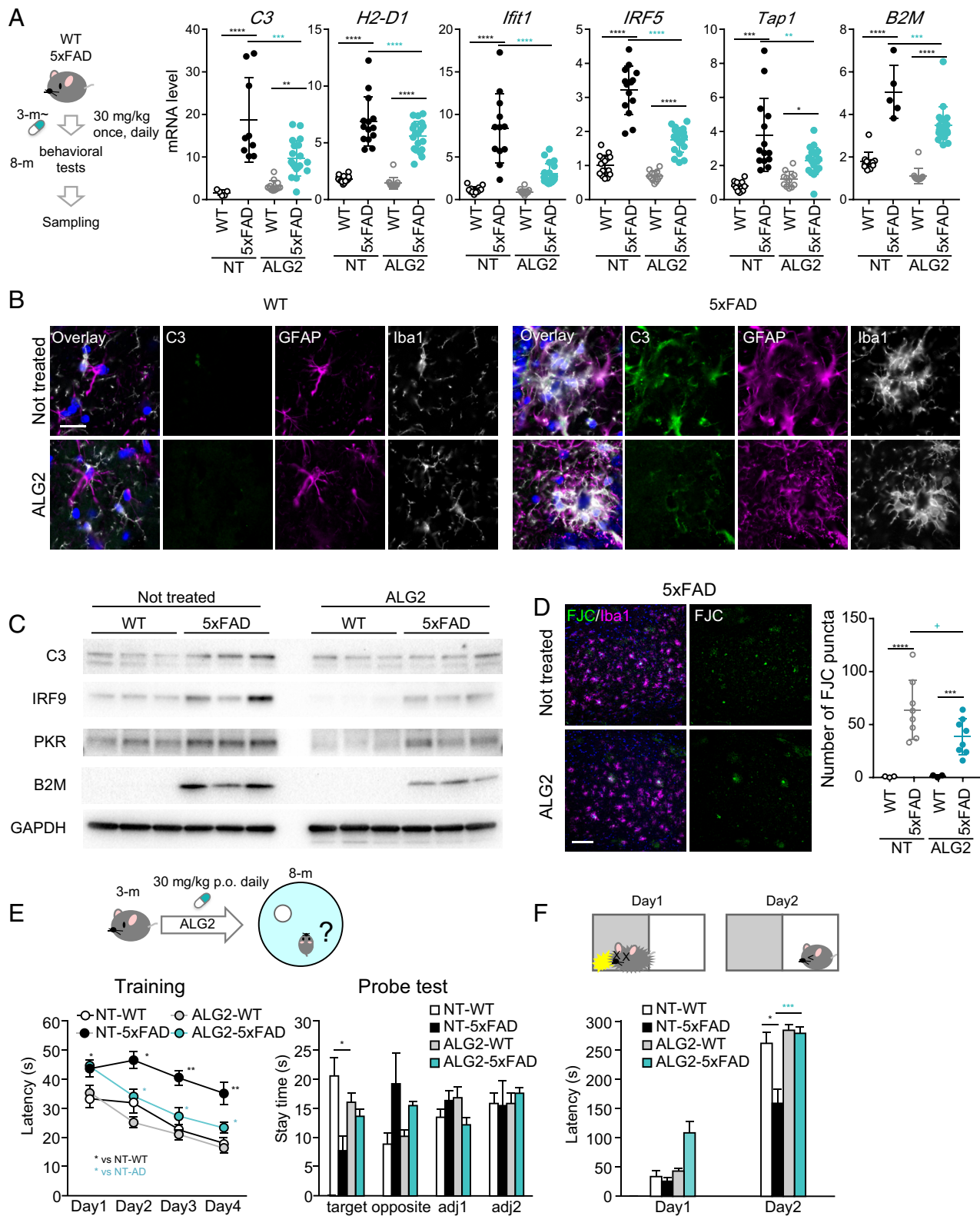


Fig. 5. Potentiating the Nrf2 pathway can suppress the neuroinflammation-triggered neurotoxic astrocytes and relieve impaired brain function in AD mouse model. (A, Left) Experimental scheme; 5xFAD mice were orally administered ALG2 daily since the age of 3 mo. Behavioral tests were performed at the age of 8 mo, followed by biochemical and pathological assessment. Right: Quantification of gene expression in the hippocampal tissues of ALG2-administered mice. Error bars indicate SEM. * $P < 0.05$, ** $P < 0.01$, *** $P < 0.001$, and **** $P < 0.0001$ (Tukey–Kramer multiple comparison test) Age: 10 mo; NT-WT: $N = 10$, NT-5xFAD: $N = 12$, ALG2-WT: $N = 12$, ALG2-5xFAD: $N = 19$. (B) Representative images of the hippocampal tissues from 5xFAD mice with or without ALG2-treatment. (Scale bar, 20 μm .) (C) Hippocampal tissues were subjected to western blot analysis using the indicated antibodies. Box plots at right indicate the quantification of the band intensities. (D, Left) Representative images of the subiculum from 5xFAD mice treated with or without ALG2. (Scale bar, 100 μm .) Right: Evaluation of the number of FJC puncta in the subiculum area. **** $P < 0.001$, *** $P < 0.0001$, and + $P = 0.10$ (Tukey–Kramer multiple comparison test). (E, Upper) Experimental scheme for the Morris water test. Lower: The latency to reach the goal was assessed from the training session. The probe test was performed for 60 s without a goal, and the time to stay in the quadrant containing the goal was measured. (F, Upper) Experimental scheme of the passive avoidance test. Day 1: mice underwent the foot shock when they entered the dark room. Day 2: the time to enter the dark room was measured. Lower: Evaluation of latency to enter the dark room. * $P < 0.01$ and *** $P < 0.001$.

the astrocytes surrounding the amoeboid-shaped microglia, which gathered around the A β -plaque regions in the brain tissue samples of 5xFAD mice (Fig. 5 B, *Right Upper*). Moreover, the up-regulated expression of C3 was suppressed upon ALG2 administration in the 5xFAD mice (Fig. 5 B, *Right Lower*). The expression levels of C3, IRF9, PKR, and B2M were down-regulated in the hippocampal tissues of the 5xFAD mice treated with ALG2, which was evaluated using western blotting analysis (Fig. 5C). We histochemically detected and quantified the neurodegeneration using Fluoro-Jade C (FJC) which specifically binds to and helps visualize the damaged neurons. Consequently, we found that the number of FJC puncta was reduced in the subiculum of mice treated with ALG2 (Fig. 5D). Thus, ALG2 administration successfully suppressed the conversion of neurotoxic reactive astrocytes and rescued the neurodegeneration caused by neuroinflammation in 5xFAD mice.

To examine whether the potentiation of the Nrf2 pathway plays a central role in rescuing impaired cognitive functions, spatial learning was assessed using the Morris water maze paradigm (Fig. 5E, scheme). The 5xFAD mice exhibited a slower learning curve during the training session than the WT mice. However, the mice administered with ALG2 exhibited accelerated learning curve, close to that of the WT mice in the training session; compared to the non-treated AD mice, ALG2-treated mice exhibited improved performance in the probe test (Fig. 5E). Improved cognition was further confirmed by the passive avoidance test where the animals learned to not enter the dark room owing to electrical foot shock (Fig. 5F). Thus, our data strongly suggest that activation of the Nrf2 pathway can suppress the gene expression and functions of reactive astrocyte and rescue the impaired brain functions of 5xFAD mice.

Discussion

In this study, we report that Nrf2 inhibits the production of neurotoxic reactive astrocytes by suppressing the recruitment of p65 upon neuroinflammatory stimulation and that ALG2, a therapeutic potentiating the Nrf2 axis, rescues cognitive impairment in 5xFAD mice. Thus, we identified Nrf2 is a key player involved in the functional determination of neurotoxic reactive astrocytes and is a potential therapeutic target for the treatment of neurodegeneration caused by neuroinflammation (Fig. 6).

Nrf2 is known to suppress inflammation, and the results of this study validate that Nrf2 also suppresses p65 recruitment in astrocytes. The role of Nrf2 in astrocytes was elucidated using the Nrf2 KO 5xFAD mouse model, which exhibited exacerbated upregulation of reactive astrocyte marker genes (Fig. 1 B–D), whereas the expression levels of cytokines and chemokines were in a similar range regardless of the presence or absence of *Nrf2* in 5xFAD mice (*SI Appendix, Fig. S1A*). In addition, ALG2 treatment theoretically promotes the Nrf2 pathway in not only astrocytes but also microglia as reported previously (15). Upon ALG2 treatment, the expression of IL-1 α was reduced, whereas TNF α and C1q expression was not affected (*SI Appendix, Fig. S8*). These results suggest that the suppressive functions of Nrf2 manifest more in astrocytes than in microglia, at least in the 5xFAD mouse model, to regulate the functions of reactive astrocytes. Moreover, Nrf2 could be broadly involved in the regulation of neuroinflammation because the Nrf2-encoding gene *Nfe2l2* is one of the up-regulated TFs as per the TF network-based analysis of a nonamyloidosis AD model (PS19 tau transgenic mice) (21). Furthermore, previous ChEA Enrichr analyses revealed *NFE2L2*/Nrf2 as overlapping signatures of astrocytes from both tauopathy MAPT^{P301S} and β -amyloidopathy APP/PS1 models (22). These data and our results support Nrf2 as a potential target to rescue various disease conditions caused by neuroinflammation. Indeed, the protective role of Nrf2 in astrocytes has been shown in mouse models of ALS (23), Parkinson's disease (24), and cerebral hypoperfusion (25) with the astrocyte-specific *Nrf2* transgene. In addition, since C3 expression in the retina of patients with AD has been proposed as an AD biomarker for early diagnosis (26), the strategy targeting astrocytes by potentiating the Nrf2 pathway could lead to the development of diagnostic markers and therapeutics for neurodegenerative disorders.

In this study, nascent RNA-seq analysis revealed expression of the neurotoxic reactive astrocyte marker genes in astrocytes upon neuroinflammatory stimulation, which are involved in antigen processing (*Tap1*) and presentation (*H2-T23*, *H2-D1*, and *B2m*) and IFN-induced GTPases (*Gbp2*, *Gbp3*, *Gbp3*, *Irgm1*, and *Iigp1*) (Fig. 4). It is noteworthy that these gene expression profiles overlapped with those of DAA identified using single-nucleus RNA-seq in 5xFAD mice (20) which have been shown to partially overlap with reactive astrocytes in our analyses (*SI Appendix, Fig. S6*), and with

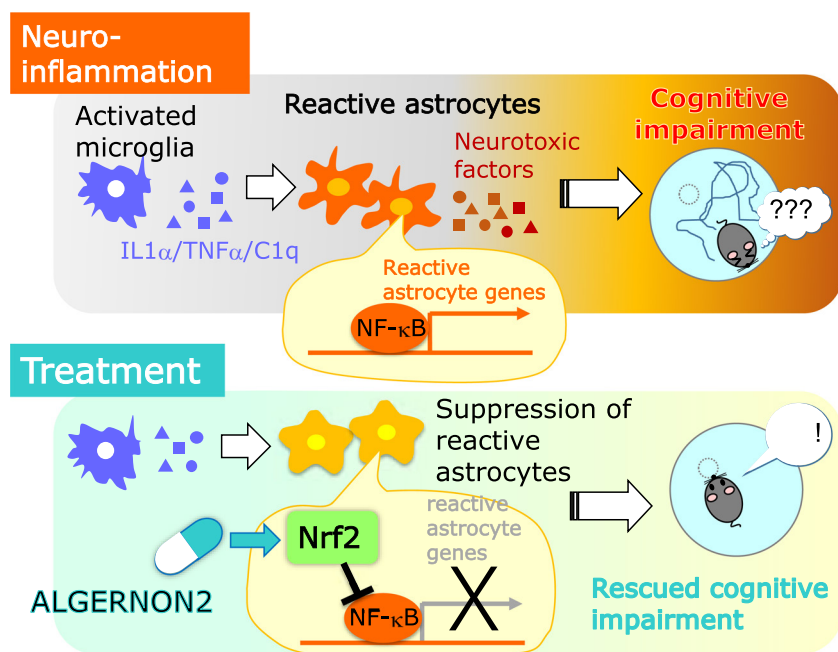


Fig. 6. Mode of action of astrocyte-targeting therapy. *Top:* In neuroinflammatory conditions such as neurodegenerative disorders, cytokines released from activated microglia induce neurotoxic reactive astrocytes via NF- κ B, resulting in impaired brain functions. *Bottom:* Treatment with ALGERNON2 can suppress reactive astrocyte conversion through Nrf2 potentiation, leading to rescued cognitive impairment in 5xFAD mice.

“cluster 8” identified using scRNA-seq in the brain of LPS-injected mice (27). The nascent RNA-seq approach enabled us to recapture the changes in the expression of genes, especially those related to IFN response occurring within neuroinflammatory astrocytes. Because these subtype-specific changes have been confirmed in several disease models, such as AD, experimental autoimmune encephalomyelitis, and acute stab wound (27), our finding that the gene expression changes can be reversed by enhancing the Nrf2 expression or activities makes Nrf2 a potential therapeutic candidate for drug development against these neurodegenerative disorders. Furthermore, it is particularly implicative that the IFN-I responses, which normally function as a part of the immune defense system against viral infections, but are also found in brains of aged humans, would suggest their negative influence on brain function (28). Moreover, normal aging has been reported to induce A1-like astrocyte reactivity (29). Mounting evidence now links chronic inflammation to aging; thus, it is even more intriguing that reactive astrocytes could likely be the source of IFN-I signaling in the brain upon neuroinflammatory stimulation, which has also been observed in aged brains. Targeting reactive astrocytes can not only ameliorate the impaired cognitive functions induced by neuroinflammation but also mitigate the decline of cognitive functions with aging. Thus, the approach to suppress reactive astrocyte production could lead to the development of therapeutics for incurable neurodegenerative diseases.

Materials and Methods

Animals. 5xFAD transgenic mice were obtained from Jackson Laboratories (Bar Harbor, ME). Nrf2 KO mice (RBRC01390) were obtained from the RIKEN BioResource Research Center (Tsukuba, Japan) with kind approval from Yamamoto (Tohoku University) (10).

Astrocyte Culture Preparation. To obtain primary astrocyte cultures, mixed glial cells were isolated from cortices of murine pups, and after the cultures reached full confluence, the microglia were removed by Cd11b-positive selection (Miltenyi Biotec, Bergisch Gladbach, Germany); the remaining cells were passaged once and then

- M. V. Sofroniew, Astrocyte reactivity: Subtypes, states, and functions in CNS innate immunity. *Trends Immunol.* **41**, 758–770 (2020).
- S. A. Liddelow *et al.*, Neurotoxic reactive astrocytes are induced by activated microglia. *Nature* **541**, 481–487 (2017).
- K. A. Guttenplan *et al.*, Knockout of reactive astrocyte activating factors slows disease progression in an ALS mouse model. *Nat. Commun.* **11**, 3753 (2020).
- S. P. Yun *et al.*, Block of A1 astrocyte conversion by microglia is neuroprotective in models of Parkinson's disease. *Nat. Med.* **24**, 931–938 (2018).
- J. S. Park *et al.*, Blocking microglial activation of reactive astrocytes is neuroprotective in models of Alzheimer's disease. *Acta Neuropathol. Commun.* **9**, 78 (2021).
- Q. Zhang, M. J. Lenardo, D. Baltimore, 30 years of NF-kappaB: A blossoming of relevance to human pathobiology. *Cell* **168**, 37–57 (2017).
- B. Kaltschmidt, M. Uherek, B. Volk, P. A. Baeuerle, C. Kaltschmidt, Transcription factor NF-kappaB is activated in primary neurons by amyloid beta peptides and in neurons surrounding early plaques from patients with Alzheimer disease. *Proc. Natl. Acad. Sci. U.S.A.* **94**, 2642–2647 (1997).
- H. Lian *et al.*, NF-kappaB-activated astroglial release of complement C3 compromises neuronal morphology and function associated with Alzheimer's disease. *Neuron* **85**, 101–115 (2015).
- R. Brambilla *et al.*, Inhibition of astroglial nuclear factor kappaB reduces inflammation and improves functional recovery after spinal cord injury. *J. Exp. Med.* **202**, 145–156 (2005).
- K. Itoh *et al.*, An Nrf2/small Maf heterodimer mediates the induction of phase II detoxifying enzyme genes through antioxidant response elements. *Biochem. Biophys. Res. Commun.* **236**, 313–322 (1997).
- E. Kobayashi, T. Suzuki, M. Yamamoto, Roles nrf2 plays in myeloid cells and related disorders. *Oxid. Med. Cell Longev.* **2013**, 529219 (2013).
- E. H. Kobayashi *et al.*, Nrf2 suppresses macrophage inflammatory response by blocking proinflammatory cytokine transcription. *Nat. Commun.* **7**, 11624 (2016).
- N. G. Innamorato *et al.*, The transcription factor Nrf2 is a therapeutic target against brain inflammation. *J. Immunol.* **181**, 680–689 (2008).
- A. Jazwa *et al.*, Pharmacological targeting of the transcription factor Nrf2 at the basal ganglia provides disease modifying therapy for experimental parkinsonism. *Antioxid. Redox Signal.* **14**, 2347–2360 (2011).
- A. Nakano-Kobayashi *et al.*, Therapeutics potentiating microglial p21-Nrf2 axis can rescue neurodegeneration caused by neuroinflammation. *Sci. Adv.* **6**, eabc1428 (2020).
- A. Uruno *et al.*, Nrf2 suppresses oxidative stress and inflammation in app knock-in Alzheimer's disease model mice. *Mol. Cell Biol.* **40**, e00467-19 (2020).

repeated for different assays. Human iPS cell line 201B7-Ff derived from a healthy individual was obtained from RIKEN BRC. Differentiation was induced according to the manufacturer's instructions (STEMCELL Technologies, Vancouver, Canada).

ChIP-seq and Nascent RNA-seq. Astrocytes were treated with DMSO or 5 μ M SLF for 1 h and then stimulated with IL-1 α /TNF- α /IC1q (inflamm) for 4 h, and ChIP-seq and nascent RNA-seq were performed as described previously (12, 30). For nascent-RNA-seq, cells were labeled with 0.5 mM EU during the last 30 min of stimulation.

A complete description of the methods is provided in *SI Appendix*.

Study Approval. All animal experiments were reviewed and approved by the Animal Research Committee, Graduate School of Medicine, Kyoto University.

Statistical Analyses. Data obtained from more than three experiments are expressed as mean \pm SEM. Statistically significant differences were determined using a two-tailed, unpaired Student's *t* test or one-way ANOVA followed by the Tukey–Kramer comparison test.

Data, Materials, and Software Availability. The accession number for ChIP-seq and Nascent RNA-seq reported in this paper is NCBI GEO: [GSE237424](https://www.ncbi.nlm.nih.gov/geo/query/acc.cgi?acc=GSE237424) (31). All study data are included in the article and/or *SI Appendix*.

ACKNOWLEDGMENTS. We thank Ms. Keiko Wanezaki for her technical assistance, Dr. Zhi-Ming Zheng for critical reviewing and advice on the manuscript, the Medical Research Support Center (Drs. Okuno, Iida, Tanaka, and Mss Hayashi and Fukuda, and Mr. Denawa) and the Animal Facility of Kyoto University (Ms. Yamane and Dr. Nakane) for assistance and the use of their equipment, and the NGS sequencing facility of Graduate School of Biostudies for sequencing. This work was supported by Grants-in-Aid from the Japan Agency for Medical Research and Development (JP23wm0525025 to A.N.-K. and JP23bm1123004 and JP23ek0109663h0001 to A.N.-K. and M.H.) and the Ministry of Education, Culture, Sports, Science, and Technology of Japan (to M.H. and A.N.-K.).

Author affiliations: ^aDepartment of Anatomy and Developmental Biology, Graduate School of Medicine, Kyoto University, Kyoto 606-8501, Japan; ^bDepartment of Drug Discovery for Lung Diseases, Graduate School of Medicine, Kyoto University, Kyoto 606-8501, Japan; ^cThe Hakubi Center for Advanced Research and Radiation Biology Center, Graduate School of Biostudies, Kyoto University, Kyoto 606-8501, Japan; and ^dInstitute of Laboratory Animals, Graduate School of Medicine, Kyoto University, Kyoto 606-8501, Japan

- G. Bahn *et al.*, NRF2/ARE pathway negatively regulates BACE1 expression and ameliorates cognitive deficits in mouse Alzheimer's models. *Proc. Natl. Acad. Sci. U.S.A.* **116**, 12516–12523 (2019).
- H. Oakley *et al.*, Intraneuronal beta-amyloid aggregates, neurodegeneration, and neuron loss in transgenic mice with five familial Alzheimer's disease mutations: Potential factors in amyloid plaque formation. *J. Neurosci.* **26**, 10129–10140 (2006).
- C. Escartin *et al.*, Reactive astrocyte nomenclature, definitions, and future directions. *Nat. Neurosci.* **24**, 312–325 (2021).
- N. Habib *et al.*, Disease-associated astrocytes in Alzheimer's disease and aging. *Nat. Neurosci.* **23**, 701–706 (2020).
- A. Litvinchuk *et al.*, Complement C3aR inactivation attenuates tau pathology and reverses an immune network deregulated in tauopathy models and Alzheimer's disease. *Neuron* **100**, 1337–1353.e5 (2018).
- Z. Jiwaji *et al.*, Reactive astrocytes acquire neuroprotective as well as deleterious signatures in response to Tau and A β pathology. *Nat. Commun.* **13**, 135 (2022).
- M. R. Vargas, D. A. Johnson, D. W. Sirkis, A. Messing, J. A. Johnson, Nrf2 activation in astrocytes protects against neurodegeneration in mouse models of familial amyotrophic lateral sclerosis. *J. Neurosci.* **28**, 13574–13581 (2008).
- P. C. Chen *et al.*, Nrf2-mediated neuroprotection in the MPTP mouse model of Parkinson's disease: Critical role for the astrocyte. *Proc. Natl. Acad. Sci. U.S.A.* **106**, 2933–2938 (2009).
- E. Sigfridsson *et al.*, Astrocyte-specific overexpression of Nrf2 protects against optic tract damage and behavioural alterations in a mouse model of cerebral hypoperfusion. *Sci. Rep.* **8**, 12552 (2018).
- A. Grimaldi *et al.*, Neuroinflammatory processes, A1 astrocyte activation and protein aggregation in the retina of Alzheimer's disease patients, possible biomarkers for early diagnosis. *Front. Neurosci.* **13**, 925 (2019).
- P. Hasel, I. V. L. Rose, J. S. Sadick, R. D. Kim, S. A. Liddelow, Neuroinflammatory astrocyte subtypes in the mouse brain. *Nat. Neurosci.* **24**, 1475–1487 (2021).
- K. Baruch *et al.*, Aging-induced type I interferon response at the choroid plexus negatively affects brain function. *Science* **346**, 89–93 (2014).
- L. E. Clarke *et al.*, Normal aging induces A1-like astrocyte reactivity. *Proc. Natl. Acad. Sci. U.S.A.* **115**, E1896–E1905 (2018).
- A. Canela *et al.*, Genome organization drives chromosome fragility. *Cell* **170**, 507–521.e18 (2017).
- A. Nakano-Kobayashi, A. Canela, T. Yoshihara, M. Hagiwara, Astrocyte-targeting therapy rescues cognitive impairment caused by neuroinflammation via the Nrf2 pathway. NCBI GEO. <https://www.ncbi.nlm.nih.gov/geo/query/acc.cgi?acc=GSE237424>. Deposited 14 July 2023.